

Effects of Hydrostatic 2nd Kind Residual Stresses and of Carbon Partitioning During Martensitic Quenching of Low Alloy Steel

Jeremy Epp

Stiftung Institut fuer Werkstofftechnik, University of Bremen, Badgasteiner Str. 3, Bremen, Germany

epp@iwt-bremen.de

Keywords: In-situ XRD, Retained Austenite, Carbon Partitioning, Hydrostatic Stress, Triaxial Stress State

Abstract. In situ X-ray diffraction measurements were performed at the ESRF in Grenoble, France during quenching of two steel grades: the ball bearing steel AISI52100 and the case hardening steel AISI5120. Diffraction frames were recorded during the complete heat treatment cycles and analyzed in order to determine the temperature- and time-dependent evolution of phase contents and lattice parameters. In the case of the AISI52100 with austenitizing at high temperature, the generation of high compressive hydrostatic stresses of 2nd kind was determined. In the case hardening steel, the dominating effect is a carbon enrichment of the austenite accompanied by the generation of compressive stresses. For the ball bearing steel austenitized at low temperature, both effects take place.

Introduction

Martensitic transformation in steels has now been investigated for more than 100 years [1] The interest in martensitic transformations is still very high as numerous industrial applications use this transformation to improve wear, mechanical and fatigue properties of parts in engineering components [2]. Moreover, new interest on fundamentals of martensitic transformations appeared in the last decades with the development of computer simulation, where kinetics, distortions and other phenomena have to be well described to reach reliable simulation results.

In situ X-ray diffraction analysis has become a powerful method of materials characterization stimulated by constant advances in instrumentation and data processing. This method allows obtaining time-resolved quantitative information about every single phase present in the investigated material.

In the present study, in situ X-ray diffraction experiments were performed with synchrotron X-ray radiation at ESRF on beamline ID11 during heat treatment of two low alloy steels with varying parameters. Different carbon contents in solution were set in hypereutectoid steel, leading to changing behaviors during quenching. Diffraction frames were recorded during the complete heat treatment cycles and analyzed to determine the temperature- and time-dependent evolution of phase contents and lattice parameters. Based on the data, different effects were investigated during quenching.

Experimental methods

Materials. A typical ball bearing steel 100Cr6 (AISI 52100) and a carburizing steel grade 20MnCr5 (AISI 5120) were investigated. The chemical composition of the 100Cr6 steel is Fe-0.95C-1.45Cr-0.44Mn-0.21Si-0.11Ni-0.10Cu-0.05Mo-0.01P-0.005S-0.004Al Mass-% while the chemical composition of the 20MnCr5 steel is as follows: Fe-0.204C-1.35Mn-1.02Cr-0.23Si-0.011S-0.03Mo-0.1Ni-0.03Al-0.1Cu Mass-%. The initial microstructure of the 100Cr6 steel exhibits a ferritic matrix with globular carbides while the steel grade 20MnCr5 presents a ferrite/pearlite microstructure with a banded morphology. The width of the ferrite/pearlite bands is about 25 μm .

In-situ X-ray diffraction experiments. In situ X-ray diffraction experiments were performed at the European Synchrotron Radiation Facility (ESRF) in Grenoble, France, on beamline ID11. The experiments were executed with a heating device (ETMT, Instron) allowing a controlled heating of samples with different section of 1.5 mm with a length of 40 mm by resistivity. Following heat treatment cycle was used for both steel grades: heating with a rate of 5 K/s up to different austenitizing temperature (T_a) between 800 °C and 940 °C followed by a soaking time of 15 min and quenching to room temperature (RT). The cooling rates led to a $t_{8/5}$ time around 2.5 s. Constant argon purging was used to avoid oxidation of the surface. The temperature was controlled by a type K thermocouple welded on the surface of the samples. During the entire heat treatment cycle, diffraction frames were recorded in transmission mode with a FRELON camera using an exposition time of 0.7 seconds for each frame during quenching with additional time for read-out of 0.1 s. The beam energy was 71 keV and the beam size was set at maximum (100 μ m high and 300 μ m width). The recorded frames were integrated with the program Fit2d and then analyzed with the Rietveld refinement software TOPAS© (Bruker-AXS). Detailed description of the experimental method and data analysis can be found in [3].

Results and discussion

Phase transformations during quenching.

After integration of the 2d-diffraction frames and analysis of the standard intensity-vs 2θ diffraction patterns by the Rietveld method, the evolution of phase content could be precisely described. Fig. 1 shows the evolution of austenite content during quenching for different initial austenitizing temperatures of the 100Cr6 material and for one 20MnCr5 sample austenitized at 900 °C. In the case of the 100Cr6, changing amount of undissolved carbides (Fe_3C) remains in the microstructure after austenitizing depending on the temperature, as expected. The kinetics of the martensitic transformation is well described. After quenching, the amount of retained austenite present in the 100Cr6 samples is 9, 14, 21 and 30 Mass-% for the austenitizing temperatures 825, 870, 905 and 940 °C respectively, while the 20MnCr5 steel exhibits about 5 Mass % retained austenite. In the case of the 20MnCr5, small quantity of bainite formed above M_s (about 10 Mass-%).

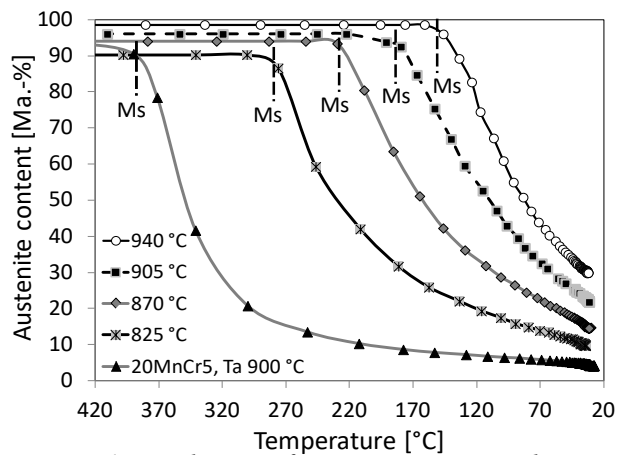


Figure 1: Evolution of austenite content during quenching of 100Cr6 samples with 4 austenitizing temperatures and a 20MnCr5 sample

Evolution of lattice parameters. From the Rietveld refinements, the lattice parameters of all present phases could be extracted. For martensite a nearly linear contraction with decreasing temperature could be observed. On the other hand, the evolution of austenite lattice parameter during cooling exhibits non-linear evolution for all experiments. The austenite lattice parameters are plotted in Fig. 2a as a function of the temperature during quenching of the considered four 100Cr6 samples and one 20MnCr5 sample. With increasing austenitizing temperature for 100Cr6 (corresponding to an increasing carbon content in solution), the lattice parameters are shifted to higher values, as expected. The thermal contraction is linear with decreasing temperature and almost parallel for all experiments until M_s is reached. During further cooling, it can be observed that for the 100Cr6 samples, a change of slope takes place with an accelerated decrease towards room temperature while the 20MnCr5 sample exhibits the opposite effect: a non-linear decrease with continuously decreasing slope takes place below M_s .

In order to observe these changes of slope during cooling, the presented data were corrected by the respective linear contraction taking place above M_s ($\Delta a = a^{\text{measured}} - a^{\text{thermal}}$) and plotted again as a function of the temperature (Fig. 2b). All values are close to 0 with small scattering

until Ms is reached. During further cooling, the continuous decrease previously observed for the 100Cr6 samples can be clearly seen, while the 20MnCr5 sample exhibits a strong increase.

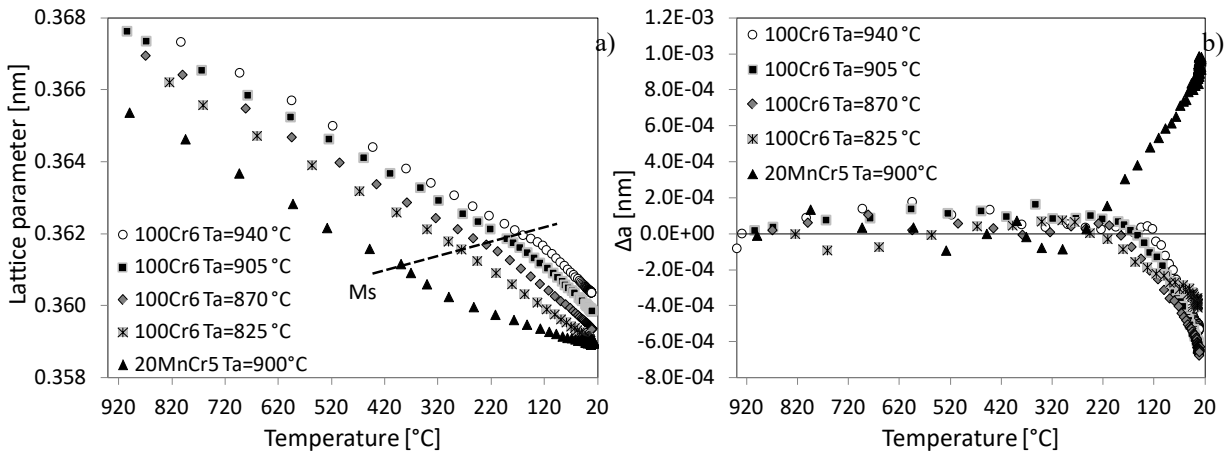


Figure 2: a) Evolution of austenite lattice parameter during quenching of 100Cr6 and 20MnCr5 sample; b) Deviation of the measured austenite lattice parameter from the extrapolated linear thermal contraction

Generation of hydrostatic stresses in austenite. Few studies can be found in the literature about residual stresses in retained austenite during or after quenching of steel. Several authors describe the residual stress state within retained austenite existing at room temperature as a hydrostatic residual stress state under high compressive stresses [4- 6]. The reason for this is a very large volume expansion associated with the martensitic transformation (close to 3%). Of course, due to shear-processes during the martensitic transformation, local residual stresses will not be purely hydrostatic in a single austenite region. However, XRD techniques give average information of thousands of “grains” and therefore the average information contained in the measured volume could be predominantly hydrostatic. In the literature, two different sets of data concerning the evolution of austenite lattice parameter at room temperature as a function of the carbon content can be found: the one based on room temperature measurements after quenching (retained austenite) and the one based either on high temperature measurements of austenite with thermal expansion correction or on Mn-/Ni-stabilized austenite at RT. From the literature data, equations were developed based on the room temperature measurements ($a^{RT}=0.3556 + 0.00443 \times \% C$) and on the high temperature measurements ($a^{stress-free}=0.3573 + 0.00327 \times \% C$) with %C in Mass.-% [4]. It can be assumed that difference between the high temperature data and the retained austenite at room temperature should be due to generation of hydrostatic residual stresses caused by the large transformation strain.

Both equations from the literature can be used to quantify the possible existing hydrostatic residual stress state in retained austenite depending on the carbon content in solution. If it is assumed that the high temperature lattice parameters describe the stress-free state while the equation based on room temperature measurements represents the retained austenite under stress after quenching, Eq. 1 can be used to calculate the corresponding strain (ϵ^{RA}) in retained austenite. The resulting hydrostatic residual stresses at room temperature can be calculated by Eq. 2 with $E^{RA}=207$ GPa and $\nu^{RA}=0.28$.

$$\epsilon^{RA} = \frac{\Delta a}{a^{stress-free}} = \frac{a^{RT} - a^{stress-free}}{a^{stress-free}} \quad (1)$$

$$\sigma^{RA} = \epsilon^{RA} \times \frac{E^{RA}}{(1 - 2\nu^{RA})} \quad (2)$$

The evolution of the literature data of the stress-free lattice parameter of retained austenite ($a^{stress-free}$) and of the lattice parameter of retained austenite after quenching (a^{RT}) depending on the carbon content in solution is presented in Fig. 3a. From these theoretical evolutions, it can be observed that at values close to 1.4 Mass-% C both lattice parameters are almost similar and with decreasing carbon content, the gap is increasing continuously. From these data and together with equations 1 and 2, resulting theoretical hydrostatic residual stresses were calculated and plotted in

Fig. 3b. At 1.4 Mass-% C, the residual stresses are close to 0. With decreasing carbon content, the theoretical values go to always increasing compressive residual stresses. For 0 % C a theoretical value of -2200 MPa is obtained.

The experimental data collected at RT within the frame of the present study were then used to calculate hydrostatic residual stresses in retained austenite based on equations 1 and 2 using the stress-free lattice parameter from the literature and plotted in Fig. 3b. It can be observed that the experimental values can be divided into two zones. For %C > 0.8 Mass.-% the values are close to the theoretical line with values between -750 MPa to -350 MPa, but with a slight shift. In previous papers, these values have been confirmed and it has been demonstrated that the strong decreasing austenite lattice parameter below Ms (Fig. 2) is due to the generation of strong hydrostatic compressive stresses due to the martensitic transformation with a continuous evolution during cooling [3, 7]. Moreover, the hydrostatic nature of the stresses could also be demonstrated by tensor measurements [3, 7].

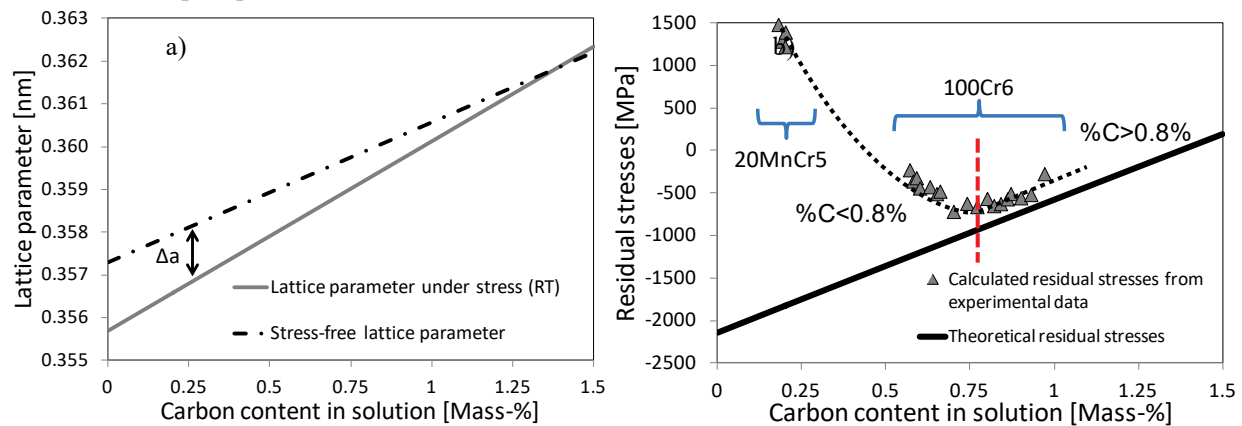


Figure 3: a) Evolution of the stress-free ($a^{stress-free}$) and the retained austenite lattice parameters (a^{RT}) as a function of the carbon content in solution (data from the literature); b) theoretical hydrostatic residual stresses in austenite (black line) and values calculated from present experimental data (triangles)

When the carbon content in is below 0.8 Mass-% a continuous deviation of the experimental values from the theoretical line can be observed. In previous publications, it has been demonstrated that in the 20MnCr5 steel a carbon enrichment of the austenite takes place during martensitic transformation leading to a carbon content of more than 0.5 Mass.-% in austenite at room temperature [3, 8]. Similar effects of carbon enrichment of austenite during quenching were already reported in the literature for low to medium carbon steels [1, 9]. Therefore, the value of hydrostatic tensile residual stresses in retained austenite for the 20MnCr5 steel in Fig. 3b is erroneous as the stress-free lattice spacing has to take into account the modified carbon content in solution. With decreasing carbon content in solution in the 100Cr6 steel, Ms increases and therefore carbon diffusion is accelerated. In the case of the 100Cr6 with low carbon content in solution, self-tempering effects will also increasingly take place with decrease C-content due to increasing Ms temperature and accelerated diffusion. As shown in [3] for the present experiments, inhomogeneous carbon distribution at nm scale could be observed by atome probe tomography and pronounced carbon depletion in martensite could be demonstrated. Therefore, a certain carbon enrichment of the austenite will also take place in the 100Cr6 steel for high Ms temperatures.

If the theoretically calculated residual stress distribution (Fig. 3b) is assumed to be the real residual stress state in retained austenite, the gap between these values and the experimentally determined values might be attributed to the effect of carbon enrichment of austenite during quenching. In order to determine the C-content in solution resulting from these assumptions, a least squares fit of the experimental data with the calculated distribution was done by implementing a dependence of the C-content in solution on the nominal C-content determined

above M_s ($\%C^{above Ms}$). Following equation giving the evolution of C-content in solution in austenite after quenching ($\%C^{RT}$) was obtained:

$$\%C^{RT} = -0.68 \times \%C^{above Ms} + 0.67 \times (\%C^{above Ms})^3 + 1.02 \quad (3)$$

The new resulting stress distribution compared to the theoretical line is shown in Fig 4a while the evolution of the resulting carbon content in retained austenite as a function of the carbon content in solution above M_s is given in Fig. 4b. Below 0.8 Mass-% C, a carbon enrichment of retained austenite after quenching is resulting. The gap between the theoretical line and the obtained behavior is continuously increasing with decreasing carbon contents. Carbon contents in retained austenite up to 1.0 Mass-% C are obtained after quenching for 0.1 Mass-% C in solution before quenching. This is in a similar range as values that have been reported in the literature [9- 11]. However, it has to be kept in mind that the determined carbon enrichment is a first estimation based on several assumptions. Moreover, according to the considered steel grade and heat treatment, variations are expected to occur.

Based on these results, it seems that carbon partitioning from martensite to retained austenite during quenching can occur for carbon contents in solution above M_s below 0.8 Mass-% C for the given cooling condition. The resulting carbon enrichment of the austenite increases for decreasing carbon contents in solution. Superimposed to this, high hydrostatic compressive residual stresses are present in retained austenite after quenching. For carbon contents in solution between 0.1 and 1 Mass-% C, compressive residual stresses in the range of -500 and -2000 MPa are resulting.

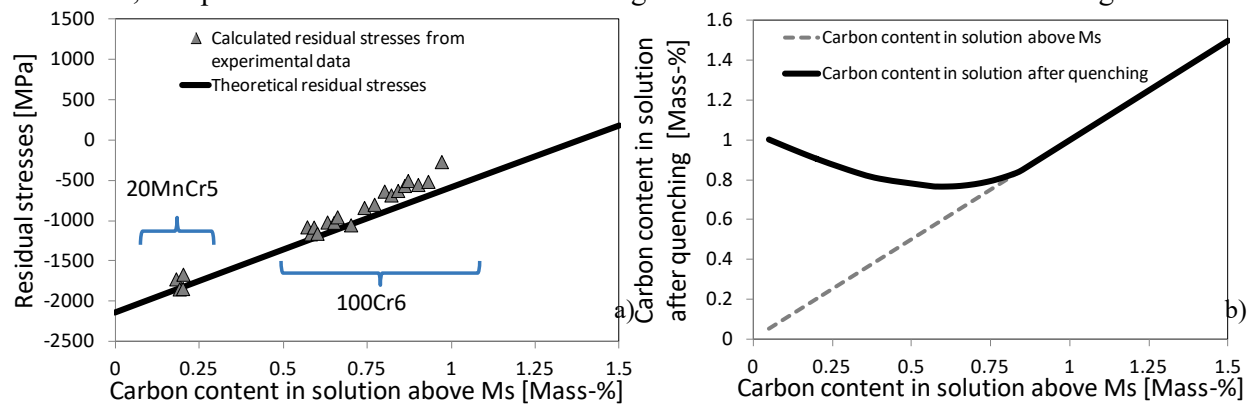


Figure 4: a) Evolution of hydrostatic residual stresses in retained austenite recalculated based on the increased carbon content in solution after quenching given in b; b) Evolution of fitted carbon content in solution in retained austenite after quenching depending on the original carbon content in solution above M_s

Based on the present results and on the in situ experiments, it is possible to determine the development of residual stresses in austenite during cooling. For experiments with carbon content in solution above 0.8 Mass-%, no carbon enrichment in austenite occurs. Therefore, a linear extrapolation of the austenite lattice parameter measured at temperatures above M_s , down to room temperature can be used to obtain the stress free lattice parameter. For the experiments with carbon content in solution below 0.8 Mass-%, the carbon contents at RT obtained from Fig. 4a can be used as end value. A specific evolution between the nominal carbon content at M_s and the final increase C-content at RT has been taken into account and is described in [3]. The stress calculations were performed by using Eq. 1 and 2 during cooling, taking into account the temperature-dependent changes of elastic properties as given in [3]. The evolutions of hydrostatic stresses in austenite during cooling are presented in Fig. 5. It can be observed that for the experiments made with the 100Cr6 steel, the increase of compressive stresses is very moderate at the beginning of the transformation, in particular for the experiments with austenitizing above 900 °C. After certain undercooling the stresses increase continuously with decreasing temperature until room temperature is reached. Towards room temperature it can be observed that small cooling steps lead to a large increase of the compressive stresses. This is also pronounced for the 20MnCr5 steel. However, it should be

remarked that especially for the experiments conducted with 20MnCr5 samples, the assumed evolution of the stress-free lattice parameters is subjected to uncertainties as the changes due to carbon enrichment might deviate from the real case.

The residual stress values reached at RT after cooling are in the range of -1800 and -750 MPa. For the experiments with austenitizing at 905 and 940 °C no carbon enrichment of the austenite is expected to occur and therefore the lattice parameter evolution above M_s was directly extrapolated to RT to determine the stress-free state. The end values reached correspond to the residual stress values obtained by using the literature data as presented in Fig. 3b what confirms that the presented results are reliable.

It should be kept in mind that a part of the results is based on assumptions concerning the carbon enrichment of retained austenite. Indeed, diffraction methods are sensitive to stresses as well as to changes of chemical composition. A proper separation of both effects is therefore almost impossible without assumptions. However, as observed with the help of the in situ experiments, as well as with more advanced techniques, clear evidences of carbon inhomogeneities were obtained [3]. Moreover, for $C > 0.8$ Mass-% C, the experimentally determined residual stresses are close to the literature values.

Summary

In situ XRD measurements were performed at the ESRF during quenching of two steel grades: 100Cr6 (AISI52100) and 20MnCr5 (AISI5120). 2D diffraction frames were recorded during the heat treatment cycles. The integrated diffraction frames were analyzed with the Rietveld-method.

By investigating the changes of austenite lattice parameter during the quenching process, it could be observed that both steel grades exhibit a non-linear evolution below M_s but in opposite direction: a slowed decrease in the case of the 20MnCr5 and an accelerated decrease for the 100Cr6 steel. For $\%C > 0.8$ Mass-%, no pronounced carbon diffusion is expected to take place and the generation of high hydrostatic compressive stresses in the austenite were determined and validated by different methods. For carbon contents below 0.8 Mass-%, carbon partitioning from martensite to austenite takes place leading to a shift of the stress-free lattice parameter. Considering a carbon enrichment which is dependent of the initial carbon content in solution, and using a least square fit based on theoretical and experimental values, a possible carbon enrichment function was determined as well as expected hydrostatic compressive residual stresses in austenite. According to these calculations, carbon enrichment takes place and reaches a maximum for initial carbon content in solution of 0.1 Mass-% with values up to 1 Mass-%. Further investigations are ongoing to verify these results.

Acknowledgments

The authors gratefully acknowledge the Deutsche Forschungsgemeinschaft (DFG) for financial support of project C01 in the Transregional Collaborative Research Centre 136 „Process Signature” as well as the ESRF for provision of synchrotron radiation facilities and financial support.

References

- [1] Olsen, G.B., Owen, W.S., Martensite, first ed., ASM International, 1992.
- [2] Metals Handbook, Vol. 1: Properties and Selection: Irons, Steels, and High-Performance Alloys, tenth ed., ASM International, 1990.
- [3] J. Epp, PhD Thesis, University of Bremen, Shaker Verlag, Aachen (2016).
- [4] L. Cheng, A. Böttger, Th.H. de Keijser, E. J. Mittemeijer, Scripta metal mat. 24 (1990) 509-514. [http://dx.doi.org/10.1016/0956-716X\(90\)90192-J](http://dx.doi.org/10.1016/0956-716X(90)90192-J)
- [5] K. Y. Golovchiner, Physics of Metals and Metallography 37-2 (1974) 126-130.
- [6] M. Villa, K. Pantleon, M. A. J. Somers, Acta Mat.65 (2014) 383–392. <http://dx.doi.org/10.1016/j.actamat.2013.11.007>
- [7] J. Epp, Adv. Mat. Res. 996 (2014) 525-531.
- [8] J. Epp, T. Hirsch, C. Curfs, Metal. Mater. Trans. 43A (2012) 2210 – 2217. <http://dx.doi.org/10.1007/s11661-012-1087-7>
- [9] T.Y. Hsu, Journal de physique IV 5-8 (1995) 351-354.